



Optimized Design of Sub-kilo Joule Dense Plasma Focus and Measurement of Neutron Yield

Ravindra Kumar Sharma¹ · Rishi Verma¹ · T. C. Kaushik¹ · Archana Sharma¹

© Springer Science+Business Media, LLC, part of Springer Nature 2020

Abstract

This paper specifically talks about optimized design strategy of sub-kilo Joule Dense plasma focus (PF) fusion device in a full-fledged systematic manner. Recently, there are many pulsed power groups working in design and development of various PF devices in the range of sub-kilo joule energy. Few of them are publishing with the optimized operating parameters for the maximum neutron yield. Most of them, talks about the estimation of PF parameters based on traditional high voltage break down mechanisms in vacuum, plasma pinch behavior and neutron generation, which are optimized for higher energy level (few kJ to MJ) PF devices. It has been very tricky and iterative way to achieve maximum neutron yield for a sub kJ PF device. A conceptual design strategy is presented for estimation of four critical PF tube parameters. These four parameters are: Anode radius, cathode radius, effective anode length and insulator length. This is very important to know these parameters, in advance of actual fabrication and plasma pinch experiments. A 400 J PF device is designed and operated at 20 kV with the help of above design strategy in single go. Maximum neutron yield is measured 50% higher with wide range of deuterium gas pressure (6–12 mbar) among sub kJ PF devices. A detailed design strategy, experimental pulsed power system development, neutron measurement and results are discussed.

Keywords Plasma focus device · Neutron generation · Plasma pinch · Pulsed power

Introduction

Dense PF device of compact sizes and operating with low energies from tens of joules to few hundred joules have found application in recent years [1–4]. A simple neutron source has always been a temptation for the users of neutrons and it becomes one of the motivations for researchers for putting the efforts to develop tabletop fusion devices. Furthermore, fast low energy devices are important for competitive neutron production under repetitive mode operation [1, 5].

It was also found that the formation of good plasma focus requires a good initial breakdown occurrence to generate a technically uniform plasma sheath. This means a plasma sheath symmetrically initiated on the insulator surface making possibility of z-pinch fusion [3].

Unfortunately, there are still no validated theoretical models to determine the dimensions of the insulator. Therefore, several tests with different insulator lengths and diameters, scanning a pressure range from 1 to 12 mbar, were necessary to determine the size of the insulator in order to obtain a homogeneous initial sheath [1]. In other Mather type PF neutron tube, The device dimensions are decided on the basis of formulated facts such as energy density parameter, drive parameter with reference to miniature PF devices and matching of the axial transit time of the plasma sheath with the quarter cycle time of the discharge circuit [6, 7]. A portable pulsed neutron source (200 J) is also reported [8]. where, drive parameter of $68 \text{ kA cm}^{-1} \text{ torr}^{-0.5}$ is used in place of $89 \text{ kA cm}^{-1} \text{ torr}^{-0.5}$ as discussed for few kJ to 100's of kJ [6, 9]. Plasma speed is also mentioned by Verma et al. [10] as $0.5\text{--}1 \times 10^5 \text{ m/s}$ in place of $1 \times 10^5 \text{ m/s}$ by authors [5, 6, 9] for sub kJ energy PF derives. Scaling law for neutron production in sub-kilo Joule devices is still matter of study [3, 5, 7]. In fact, we can question if good focusing

✉ Ravindra Kumar Sharma
rksharma@barc.gov.in

¹ HBNI, Bhabha Atomic Research Centre, Mumbai 400 085, India

can be achieved below 1 kJ, and if so which are the appropriate design criteria in this energy region [3].

In spite of all the available literature, there are several questions still waiting for answers, particularly those concerning the design strategy for estimation of four important parameters of sub kJ PF tube to generate maximum neutrons/shot for given electrical energy. Most of the experimental studies were focused in medium and large facilities from tens to hundreds of kilojoules, or small devices about some kilojoules. An area of research that is not well explored is that of the very-small low-energy plasma focus. This article is divided into two parts. The first part is focused on the design strategy of PF device in sub kilo Joule range. The second part is devoted to the development, testing and results.

Design Strategy

Neutron yield and pinching efficiency is directly influenced by design of the PF device and its operating parameters [4].

Let start from pulse power design and then finally measure x-ray and neutron yield of the developed system.

Energy Module and Discharge Current

As a first step towards the design of a PF device, It is targeted to generate 10^6 neutrons per shot from a sub kilo Joule PF device. Neutron production in a PF device is given by $Y_{4\pi} \approx 10^7 \times E^2$ as discussed [3, 11], energy stored (E , kJ) in a capacitor module. This gives the fare idea that a 400 J energy module may generate 10^6 neutrons per shot as per targeted neutron yield.

PF devices are usually operated to very high voltages, extremely higher than those strictly necessary to produce the gas breakdown. Indeed, there is a lower limit on the charging voltage of the capacitor bank due to the inductive voltage drop during the axial acceleration phase. It's quite intuitive that the variable inductance of the equivalent RLC circuit of PF system grows during the sheath motion, since the space filled by the magnetic field increases with its axial position [12]. The voltage drop related to the inductance component of the circuit is given by the second term $d(LI)/dt$ of Eqs. (1) and (2). To obtain the maximum compression effect in the focus phase, the acceleration of the current sheath should end in temporal coincidence with the first maximum of the current, roughly hundreds of kA as given in Eq. (3). Then, it follows that the maximum value of the voltage drop is mainly given by the varying inductance component, which means:

$$\frac{d}{dt}(L(t)I(t)) = L(t)\frac{dI(t)}{dt} + I(t)\frac{dL(t)}{dt} \approx I(t)\frac{dL(t)}{dt} \quad (1)$$

$$L(t) = \frac{\mu_0}{2\pi} \ln\left(\frac{b}{a}\right) Z(t) \quad (2)$$

$$V_L = I(t)\frac{dL(t)}{dt} = I(t)\frac{\mu_0}{2\pi} \ln\left(\frac{b}{a}\right) \frac{dZ(t)}{dt} \quad (3)$$

Typically the radiuses ratio lead to $\ln(b/a) \approx 0.5$ to 1, while the peak current is 0.5–1 MA; where a : anode radius and b : cathode inner radius. This gives an inductive voltage drop per axial speed of 1 kV per 1 cm/ μ s. Usually, the velocity of the current sheath varies in the 1–5 cm/ μ s for a PF tube operating in deuterium as shown in Table 1. On the other hand, it observed the focusing speed exceeds 10 cm/ μ s. Thus, from Eq. (3), it shows that the inductive voltage drop is approximately of 10 kV, which is main reason why most PF work with charging voltages in the range of 20–30 kV. One can easily calculate the capacitance (2 μ F) required to store the $E = 400$ J energy at 20 kV operating voltage as optimum value as per above discussion. Electrical circuit parameters (R & L) are so controlled to minimize their values. The measured total driver circuit inductance (\approx capacitor module + transmission line inductance + spark gap + electrical short in place of PF tube) is about 55nH. Discharging peak current (I_0) is estimated to 100 kA for a electrical circuit of 2 μ F, 20 kV, 70% of voltage reversal.

Anode Radius and Gas Pressure

There are two very important parameters, energy density and drive parameter that are used in design of PF devices. Energy density and Drive parameters are defined as $\frac{I_0}{ap^{0.5}}$ and $28E/(a^3)$, Investigation on sub kJ PF devices [4, 6–9, 13] operating in D_2 gas shows their values around $5 \cdot 10^{10}$ J/m³ and 77 ± 7 kA/cm.mbar^{0.5} respectively. First anode radius (a) is calculated as 0.6 cm from the energy density parameter. The operating D_2 gas pressure (p) is calculated as 5 mbar from drive parameter. This operating pressure is in the same range as published by other researchers in sub kJ PF devices. However, the optimized pressure for the neutron yield is experimentally obtained with pressure variation study.

Insulator Length and Cathode Radius

Insulator length and its material has been a debatable parameter to estimate as many authors have given different ways to find it. It was observed that neutron yield increased linearly with the product of the pressure and the dielectric constant [14]. But Rout et al. [15] has showed that the glass and quarts insulator show nearly the same behavior and

Table 1 Experimental parameters of various PF devices

References	Energy (J)	Voltage (kV)	Anode radius (cm)	Cathode radius (cm)	Leff. (cm)	Lins. (cm)	T/4 (ns)	Lins./V (mm/kV)	Lins/(b-a)	b/a	Axial speed (cm/us)	Yield 10^6 Neutrons/shot
Silva et al. [3]	400	30	0.6	1.55	0.7	2.1	300	0.7	2.2	2.6	2.3	1.06
Niranjan et al. [17]	500	10	0.5	2.0	6.0	2.0	1650	2.0	1.3	4.0	3.6	0.13
Silva et al. [1]	50	25	0.3	1.35	0.4	1.92	150	0.8	1.8	4.5	2.7	0.01
Milanese et al. [20]	125	16	0.75	2.1	2.2	0.7	400	0.4	0.5	2.8	5.5	1.00
Shukla et al. [21]	75	4.0	0.6	1.25	1.0	0.6	1110	1.5	0.9	2.1	0.9	–
Verma et al. [10]	200	13	0.4	1.1	2.0	0.5	370	0.4	0.7	2.8	5.4	0.01
Silva et al. [1]	32–98	20	0.6	1.35	0.5	0.5	220	0.3	0.7	2.3	2.3	0.03
Hassan et al. [22]	58–160	30	0.8	2.4	0.7	1.46	325	0.5	0.9	3.0	2.2	–
Beg et al. [23]	100	38	1.0	2.25	3.0	2.0	800	0.5	1.6	2.3	3.8	–
Hossein and Habibi [24]	3.6	15	0.13	0.72	0.45	1.3	68	0.9	2.2	5.7	6.7	–
Verma et al. [10]	170–270	13	0.6	1.5	1.7	0.5	400	0.4	0.6	2.5	4.3	–
Present paper	400	20	0.6	2.0	1.2	1.0	520	0.5	0.7	3.3	3.5	1.9
						Avg. values:		0.8	1.2	3.3	3.5	

further confirmed that the quartz turns out to be better insulator than alumina [16]. Many of the researchers experimentally found the optimum insulator length by varying the insulator length and deuterium gas pressure in the PF tube [1, 3, 5, 7, 17] and by referring comparative studies reported for enhancement of the neutron yield [5, 8]. Both the papers of the Yousefi et al. [18, 19] has shown the ratio of the insulator sleeve length to the radial distance between the electrodes, " $L_{ins}/(b-a)$ " is between 1 and 1.8 for few kJ energy to 10^7 's of kJ energy PF devices. There is no place for the sub kilo joule energy PF device in his paper. The same idea is carried to the 20 J and 2.5 J energy PF devices by Jafari et al. [4] and Goudarzi et al. [9] respectively, in sub kJ energy PF devices but could not show the neutron generation. A quantitative parameter is defined as the ratio of the insulator length with breakdown voltage as 0.5–0.8 mm/kV for sub kilo joule energy PF device as shown in Table 1. This ratio is decreased to 0.48 mm/kV, when 10 kV or lower operating voltage PF devices are dropped. An optimum length of 10 mm is inferred based on the above discussion for ID: 10 mm and OD: 12 mm quartz insulator. Cathode radius of PF tube is equally important for the smooth current sheath formation on the insulator during break down phase to pinch and rupture of the plasma column for neutron generation. Snowplow model has shown the ratio (b/a) is a constant

$c = 1.5$ to 2 presented by Lee and Serban [6] and also Tarifeño-Saldivia and Soto [5] talks about this value around $c = 2.5$ for the machines of kJ ranges. The average ratio comes out to be 3.1 as the shown in Table 1. Based on above discussion 20 mm optimum cathode radius is calculated.

Anode Length

The quarter rise time ($T/4$) of electrical discharges are typically in the range of a few microseconds (1–5 μ s) for medium and high energy range PF devices, but in the sub-kJ range miniature PF devices it is faster, typically 100 to 700 ns range. Therefore the associated plasma dynamics is much faster in comparison with conventional kJ PF devices. Stainless Steel is chosen for Anode and cathode electrodes material based on the various studies for neutron yield and recommendations [5, 8–10, 24].

The implications of this temporal regime on the behavior and performance of the discharge are not well known to researchers. Axial and radial velocity for kJ PF devices is in the range of $0.8-1 \times 10^5$ m/s and $1.5-2.5 \times 10^5$ m/s, respectively as per Serban [25]. A good research work on pinch plasma focus devices of hundreds of kilojoules to tens of joules is presented by Lee [6] and Soto [7]. There is not any clear data for the sub kilo

Joule PF devices, So an average axial and radial velocity and initial break down phase timing are inferred and used for design estimation of anode as following:

The average axial velocity is inferred from the Table 1 as 0.35×10^5 m/s and radial velocity (2.25×10^5 m/s) is reported by Serban and Lee [25]. First time researcher Jafari and Habibi [24] introduced the time duration of the break down phase (t_{br}), which looks convincing to be in the range of 25% to 40% of $T/4$ of the capacitor discharge. Therefore, effective anode length (z_a) is determined by Eq. (4). Time duration of the break down phase (t_{br}) is considered as 28% of $T/4$ of the capacitor discharge for operating voltage in the range of 20 kV and lower insulator length.

$$\frac{T}{4} = \frac{z_a}{v_a} + \frac{a}{v_r} + t_{br} \quad (4)$$

Cylindrical cathode PF device (2 μ F, 20 kV, 400 J, 55 nH and voltage reversal of 70%) is having 520 ns as the quarter period. The effective optimum SS anode length of 12 mm is calculated by considering the value of t_{br} (28% of the $T/4$ capacitor discharge time), axial velocity, radial velocity and anode radius as 146 ns, 0.35×10^5 m/s, 2.25×10^5 m/s and 6 mm, respectively using Eq. (4). Experimental testing is also performed with anode length of 16 mm, without considering above discussion and Table 1, and just used the axial velocity as 0.5×10^5 m/s in place of as 0.35×10^5 m/s and Time duration of the break down phase (t_{br}) as 30% in place of 28% of quarter period. Further, a taper is incorporated in the anode length over the last 5 mm of the anode, with 6 to 3 mm radius gradual decrement. The decrease in the anode radius should enhance the linear current density (I_0/a) and hence should increase the compression efficiency [10].

Pulsed Power Setup and Plasma Tube

PF device dimensions are decided on the basis of above discussions and Table 1. High current (100 kA) electrical pulse of a sub microseconds duration is required to operate the plasma focus. This necessity is fulfilled by the pulsed power system which mainly comprises: (1) capacitor module as energy storage, (2) triggered high voltage switch to transfer the stored energy from the energy module to the plasma focus load. (3) connections used for connecting switch to the plasma load and the capacitor, and (4) HV charger for charging the capacitor bank to a suitable voltage and a spark gap switching trigger pulse. The mentioned constituting components—capacitor bank, triggered switch and connections are supposed to have the following common characteristics: (a) low inductance and resistance, (b) ability to withstand the desired high voltage, (c) high

current carrying capacity, and (d) ability to withstand heavy mechanical stresses due to the high magnetic fields. A film-foil capacitor (2 μ F, 20 kV, 30 nH) is designed and developed in a compact size (30 cm \times 24 cm \times 12 cm, 14 kg) as 400 J energy module. Energy module (Test voltage: 22 kV, 60 s.) has coaxial electrode geometry to maintain the low circuit inductance. A field distortion triggered spark gap is employed between capacitor module and PF device load in coaxial geometry. This spark gap is operated at 20 kV, which is 90% of the self break down voltage (SBV) of 22 kV to confirm the low impedance during discharge. Triggered spark gap is operated at atmospheric pressure to maintain the OD: 70 mm and Length: 30 mm in a compact size. Design of spark switch is in such a way that an air gap (18 mm) is created between central HV electrode (SS304, OD:8 mm) of capacitor module and placement of anode of PF device with the help of M6 screws. A photograph of the complete PF system is displayed in Fig. 1. The PF system is having 450 mm(H), 240 mm(W) and 120 mm(D) as overall size. The capacitor bank is charged by a high voltage–power supply (30 kV, 20 mA) in constant current mode with of 200 V/s charging rate. A compact switching circuit [26] for triggering the spark gap is developed using ferrite toroidal core based HV pulse transformer. The primary of the pulse transformer (15 kV, 300 ns) is fed by the 600 V, 0.22 μ F capacitor discharge circuit using BTW-1200 SCR switch. Capacitor charging (on/off), spark gap triggering and pneumatic capacitor shorting device operations are carried out by a hand held compact control panel (100 mm*50 mm*30 mm) connected by a 10 m long multi-core cable.

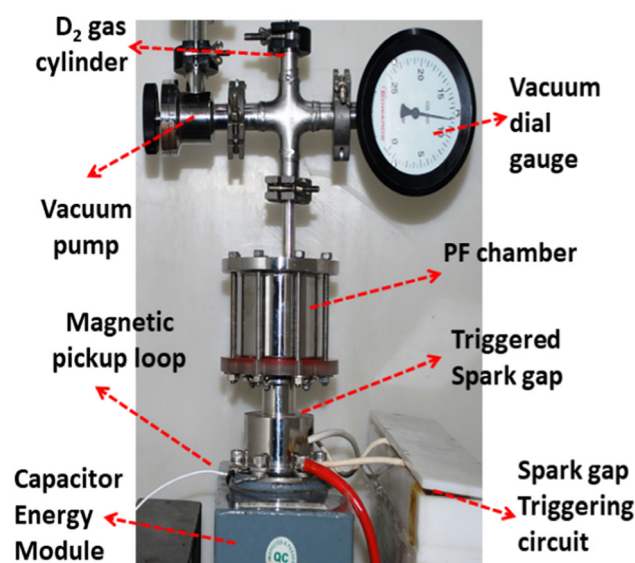


Fig. 1 Photograph of the complete PF system

Metal components of PF tube are thoroughly cleaned and dried at 70 °C for 30 min in an oven. All the components are assembled and sealed with o-ring mechanism with the help of outer SS vacuum cylindrical cover to create a vacuum chamber. KF-16 Flange (SS) is welded at the top of the PF vacuum chamber for evacuation, filling and pressure measurement of the operating gas as shown in Fig. 1. Leak detector is used to confirm the vacuum sealing and leak rate of 10^{-9} Pa m³/s is measured.

Plasma Pinch Testing and Analysis

To maximize the efficiency of PF device, it is important to match the axial transit time of the plasma sheath with the quarter cycle time of the discharge current. It is confirmed during the design of the PF tube as discussed above. The sharp dip in current derivative shows the pinch quality and indicates the higher neutron yield.

Electrical Operation and Gas Pressure Effect

PF device is first operated with hydrogen gas for electrical parameter estimation. This also confirm the effect of the operating pressure on pinch position at 20 kV charging voltage as shown in Fig. 2. Plasma pinch time (t_p) variation

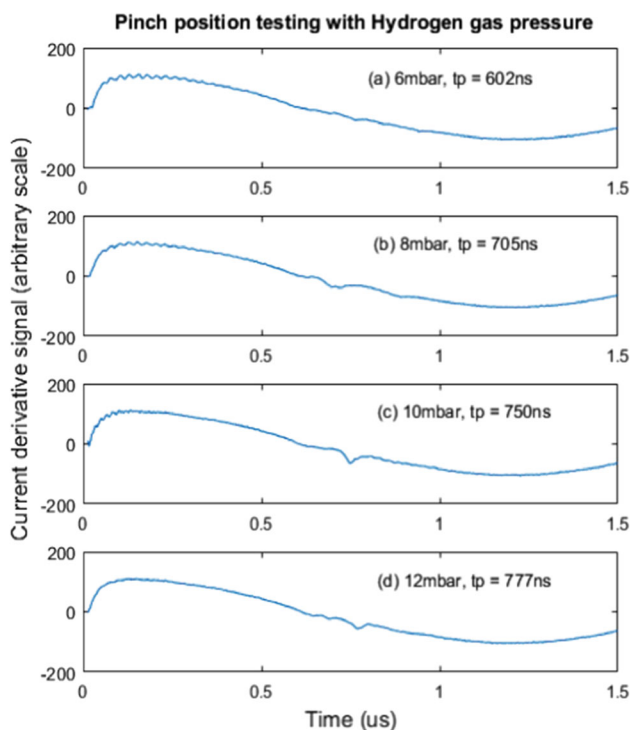


Fig. 2 Current derivative signals showing pinch position at various hydrogen gas pressure

is measured as 602 to 777 ns with 6 to 12 mbar pressure range. This increase in focusing time is noticed with the increase in gas pressure, which is consistent with previous literature work [27]. The most basic and preliminary investigation is the appearance of distinct and sharp dip/focusing peak in the current derivative signal (di/dt) for optimum operation of plasma focus device. This dip mainly indicates rapid change in plasma impedance on pinching. The variation in time to pinch (t_p) from the breakdown phase increases with the increase in operating pressure due to consequently increased load on the current sheath. The data are taken in single shot mode, for every choice of gas pressure. The gas is refreshed after every single shot during the experimental run of shots, to reduce the effect of contamination on plasma pinch quality. All the operations of PF system are operated from a distance of 10 m, to reduce the effective dose in the range of few nSv. It is also important to note that the PF system is kept inside a HDPE shield room (Wall thickness: 10 cm, size: 120 cm (L) × 120 cm (W) × 200 cm (H)) to reduce the radiation dose by x-ray and neutrons.

Time Resolved Neutron Diagnostics

This same PF setup is tested with deuterium gas for neutron generation through D–D reaction. Deuterium gas has lesser ionization energy and supports the good ionization and a sharp dip is observed in current derivative signal at the time of plasma pinch as shown in Fig. 3. Tests are performed using a scintillation detector–photomultiplier (PMT) system to register the time resolved hard X-ray (HXR) and neutron pulse. TOF detector is a NE-102 plastic scintillator (Diameter: 51 mm and Thickness: 51 mm) optically

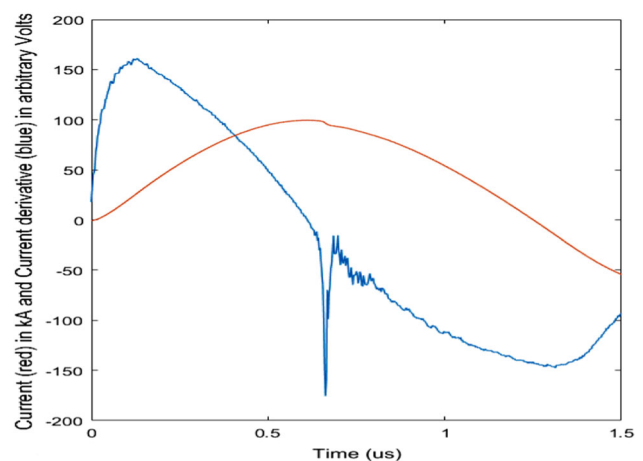


Fig. 3 Current (red) and current derivative (blue) signals at 10 mbar (Color figure online)

connected to ET 9815 PMT. A high voltage–power supply was used to provide -2200 V bias to the PMT.

PMT is surrounded by a solid mu metal and is equipped with a built-in voltage divider for negative high voltage. The electrical output is connected to the 1 GHz Digital Storage Oscilloscope (DSO) powered with battery backup system to reduce the signal noise. The scintillator–PMT system was placed at a distance of 0.5 m away from the PF device at 90° from the device vertical axis. TOF measurement is inferred from the time difference between HXR and neutron pulse shown in Fig. 4. The first negative spike represents the HXR, which reached the scintillator first followed by the neutron signal 23 ns later, which is in close agreement with 24 ns (2.45 MeV) D–D neutrons. Similarly, Lead screened PMT 1 and PMT 2 are placed at 0.5 m and 1.0 m distance, respectively. Lead sheets of 15 mm total thickness are placed in front of both PMTs to suppress the x-ray pulse emanated from the PF device and record only neutron signal. The measured time separation between the falling edges of the neutron pulses of the two PMTs is used for neutron time-of-flight estimation. The time of flight of the neutrons between the two PMTs is 23.5 ns and neutron pulse width of 12 ns as shown in Fig. 5. This is also confirming the 2.45 MeV energy of neutrons.

It is shown that the pinch life time (t_{pf}) is estimated as: $t_{pf} = 2a$, where a is in mm and t_{pf} in ns [25]. For above PF device the anode radius is 3 mm after considering the taper part as discussed above in the section “Anode Length”. So, empirically estimated pinch life time is 6 ns, which is in the same range of experimental values (10–12 ns), shows good agreement.

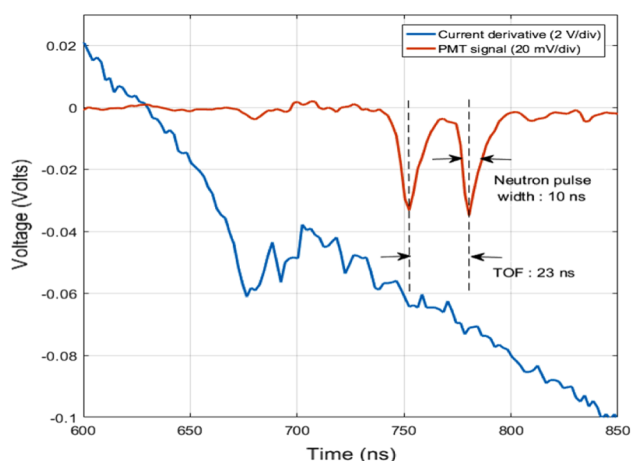


Fig. 4 Current derivative (blue) and PM tube sensor (red) signals (Color figure online)

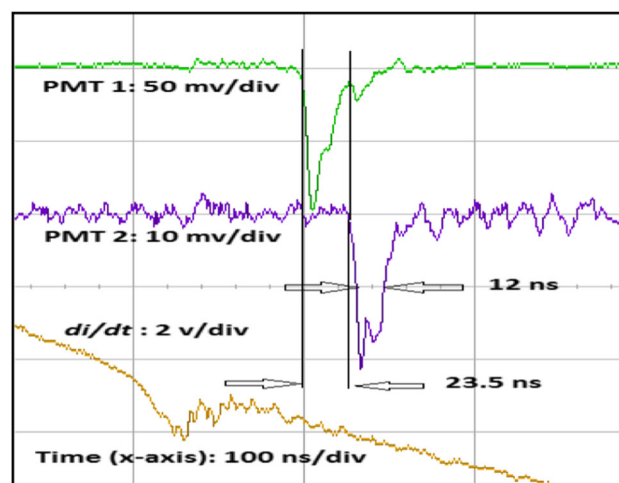


Fig. 5 Current derivative (yellow) and PM tube (green and purple) signals (Color figure online)

Neutron Diagnostics Using a ^3He Proportional Counter

Amongst all, ^3He detector is most suitable because of its high neutron (thermal) detection efficiency (typically $\sim 77\%$) and low gamma ray sensitivity [10]. Neutron yield is measured using a calibrated Helium-3 (^3He) detector tube (Dia: 25 mm and Length 300 mm with sensitivity: 30 cps/nv), which is encapsulated inside a 7 cm thick HDPE cylindrical moderator. Thickness of the moderator is precisely calculated to maximize the counting efficiency for 2.5 MeV neutron energy. ^3He detector is located at 20 cm away from the PF tube in radial direction. ^3He detector output is fed to Pre-Amp, and a typical electrical charge signal is captured as shown in Fig. 6 at operating pressure of 10 mbar. Area under curve (total charge) is calculated as 19.3 mVs and divided by the calibration factor of the ^3He detector. ^3He detector is calibrated (9.1 nVs/Neutron) by Cf-252 (3.45×10^5 Neutrons/

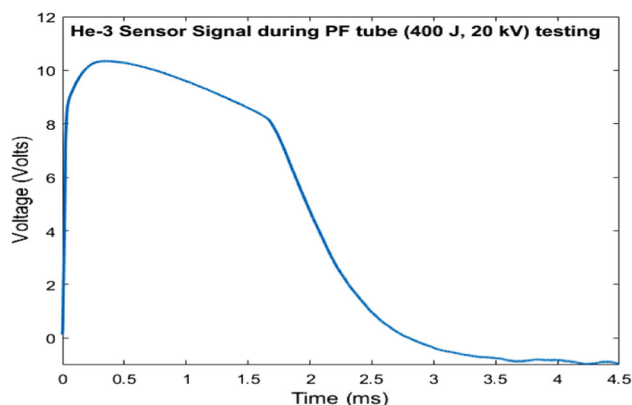


Fig. 6 He-3 Sensor signal during PF testing for Neutron yield measurement at 10 mbar pressure

s) neutron source. By this way, neutron yield (2.12×10^6 Neutrons/shot) is calculated for each shot. This method is described briefly above and in detail in [10, 28]. The maximum neutron yield: 2.4×10^6 Neutrons/shot and average maximum neutron yield: $(1.9 \pm 0.4) \times 10^6$ Neutrons/shot are measured over multiple discharges at 9 mbar and 10 mbar pressure respectively, with pressure scan from 1 mbar to 14 mbar as shown in Fig. 7. Ten shots are performed at each pressure level to generate the statistical data.

Experimental Testing of 16 mm Anode Length

Experimental testing is also performed with 16 mm in place of 12 mm anode length. Similar steps are followed as discussed above to test modified anode length of 16 mm in 20 kV, 400 J PF device. Pinch position is shifted from 745 to 810 ns with D₂ gas pressure 2.5 to 5 mbar variation. There is not any pinch formation below 2.5 mbar and above 5 mbar pressure. As shown in Fig. 8, One can easily see that the time to pinch is 745 ns (red colour) for anode length of 16 mm at 2.5 mbar compare to 620 ns (green colour) for anode length of 12 mm at 9 mbar pressure. It is very important to note that, there may be cases that one can get pinch in the current derivative waveform for 16 mm length anode as discussed above, but there are hardly or few shots could generate lower neutron yield of 10^5 – 10^6 Neutrons/shot as shown in Fig. 7. This is due to the lesser D₂ ion density at lower pressure and lower pinch current (I_p) magnitude for longer anode (16 mm) PF device. It is not always true that by changing the pressure, one can reach to the maximum neutron yield for given electrical energy for any PF tube dimensions.

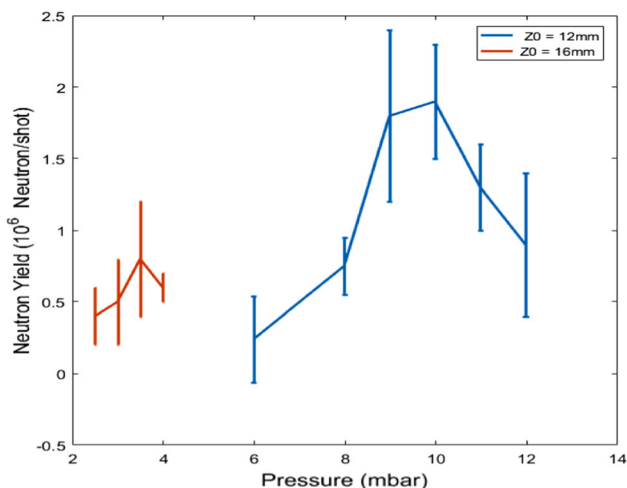


Fig. 7 Neutron yield variation for anode length of 16 mm (red) and 12 mm (blue) with pressure (Color figure online)

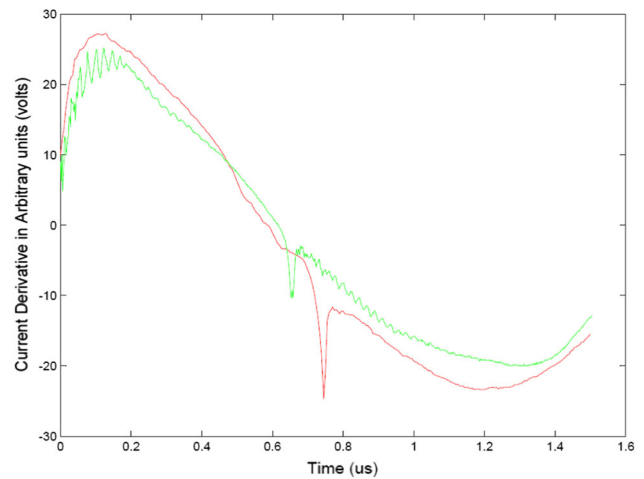


Fig. 8 Current derivative (red, tp: 745 ns) for anode length of 16 mm at 2.5 mbar and Current derivative (green, tp: 620 ns) for anode length of 12 mm at 9 mbar pressure (Color figure online)

Discussion

Scaling law [3, 11] $Y_{4\pi} \approx 10^7 \times E^2$ for present 400 J, 20 kV ($I_p = 78$ kA, $(1.9 \pm 0.4) \times 10^6$ Neutrons/shot) PF device is inferred as $Y_{4\pi} \approx 10^7 \times E^{1.8}$ due to comparatively higher neutron yield, E in kJ. This yield is also deviated from the Scaling law [12] $Y_{4\pi} \approx 8.43 \times 10^{-4} I_p^{4.59} = 0.4 \times 10^6$ Neutrons/shot for few kJ and sub kJ devices, I_p is pinch current in kA. Many research publications are available in low energy PF devices (sub kJ energy level), but no one talks in such a detail. A conceptual design strategy is presented for estimation of four critical tube parameters: Anode radius (by utilizing both energy density and drive parameter), cathode radius (by considering the avg. ratio (b/a) for only sub kJ devices), effective anode length (by utilizing break down phase and avg. axial velocity) and insulator length (by quantifying avg. ratio of insulator length to operating voltage). A tapered anode effect in plasma channels compression efficiency is always better to incorporate in the very first design of anode electrode.

Performance of the present device with higher pressure (10 mbar) operation, lower insulator length and tapered anode to 3 mm confirm higher neutron generation. Drive parameter ($106 \text{ kA/cm} \cdot \text{mbar}^{0.5}$) and energy density ($\sim 10 \times 10^{10} \text{ J/m}^3$) are slightly deviate at higher side of typical range [4, 6–9, 12] of $77 \pm 7 \text{ kA/cm} \cdot \text{mbar}^{0.5}$ and $1\text{--}10 \times 10^{10} \text{ J/m}^3$ respectively.

It is also possible to improve the neutron yield values of various publishers [1, 4, 9, 21] by just reducing the anode length of PF devices. This can be achieved by applying the above discussed design strategy and bring the pinch position close to right side of zero crossing position in current

derivative signal. Decrease in anode length increases the peak current as well as shifts the pinch position towards zero crossing point of current derivative (i.e., higher pinch current) to achieve best efficiency (higher operating pressure). These two effects (higher pinch current and pressure) enhance the ion density and temperature of the pinch plasma to generate enhanced neutron yield for the same capacitor energy. This is experimentally demonstrated by authors [3, 10, 20] through many trials (by varying anode length, insulator length, energy etc.) but in this paper systematically implemented with the four parameters design method for sub kJ PF device.

Conclusion

Step by step systematic optimized design procedure based on empirical equations and intense literature survey offers higher capabilities with minimum iterations/modifications in design and development of PF device in sub kJ range. This paper has presented the efforts to design (optimized parameters shown in Table 1) and develop a compact PF device (20 kV, 400 J). Overall size of the complete PF system is only 400 J, 12 cm × 24 cm × 45 cm, 17 kg, 56 nH circuit inductance. This is a much compact system compare to 400 J, 10^6 Neutrons/shot, 25 cm × 25 cm × 50 cm by Silva [3] and 200 J, 10^4 Neutrons/shot, 20 cm × 20 cm × 50 cm, 25 kg by Rishi [10]. Together PF tube and spark gap cost is less than US, 70 \$ and yet, experimentally showed the neutron generation in single go. Reduction in overall size with enhancement in average neutron yield $(1.9 \pm 0.4) \times 10^6$ Neutrons/shot, which is more than 50% higher average neutron yield than the same 400 J energy PF device 1.06×10^6 Neutrons/shot [3]. Higher maximum neutron yield of 2.4×10^6 Neutrons/shot among all the publishes data are clearly observed from the above discussion Fig. 7 and from Table 1 against similar energy PF devices.

This paper have been a good reply to the question raised by many researchers, such as: Silva [3] says that “If good focusing can be achieved below 1 kJ, and if so which are the appropriate design criteria in this energy region”.

Acknowledgements The authors are grateful to Shri D. Das, Director, E&I Group, BARC for his continuous support and encouragement in development of this technology. The authors also acknowledge and thank Shri V Sathian and Smt Dr M N Rao, BARC, Mumbai for their assistance at various stages of neutron yield measurement.

References

1. P. Silva, L. Soto, W. Kies, J. Moreno, *Plasma Sour. Sci. Technol.* **13**, 329 (2004)
2. S.S. Hussain, S. Ahmad, G. Murtaza, M. Zakauallah, *J. Appl. Phys.* **106**, 023311 (2009)
3. P. Silva, J. Moreno, L. Soto, L. Birstein, R.E. Mayer, W. Kies, *Appl. Phys. Lett.* **83**, 3269 (2003)
4. H. Jafari, M. Habibi, G.R. Etaati, *Phys. Lett. A* **381**, 2813 (2017)
5. A. Tarifeño-Saldivia, L. Soto, *Phys. Plasmas* **19**, 092512 (2012)
6. S. Lee, A. Serban, *IEEE Trans. Plasma Sci.* **24**, 1101 (1996)
7. L. Soto, P. Silva, J. Moreno, G. Silvester, M. Zambra, C. Pavez, L. Altamirano, H. Bruzzone, M. Barbaglia, Y. Sidelnikov, W. Kies, *Braz. J. Phys.* **34**, 1814 (2004)
8. R. Niranjana, R.K. Rout, P. Mishra, R. Srivastava, A.M. Rawool et al., *Rev. Sci. Instrum.* **82**, 026104 (2011)
9. S. Goudarzi, N. Aral, H. Babaee, A. Nasiri, A. Esmaeli, *Plasma science and applications (ICPSA)*, in *International Journal of Modern Physics: Conference Series* vol 32 (2014)
10. R. Verma, M.V. Roshan, F. Malik, P. Lee, S. Lee, S.V. Springham, T.L. Tan, M. Krishnan, R.S. Rawat, *Plasma Sour. Sci. Technol.* **17**, 045020 (2008)
11. R.K. Sharma, A. Sharma, *Rev. Sci. Instrum.* **88**, 033502 (2017)
12. M. Frignani, *Simulation of Gas Breakdown and Plasma Dynamics in Plasma Focus Devices*. Ph.D. Thesis (2007)
13. L. Soto, C. Pavez, A. Tarife, J. Moreno, F. Veloso, *Plasma Sour. Sci. Technol.* **19**, 055017 (2010)
14. F.N. Beg, M. Zakaulla, G. Murtaza, M. Beg, *Phys. Scr.* **46**, 152 (1992)
15. R.K. Rout, A.B. Garg, A. Shyam, M. Srinivasan, *IEEE Trans. Plasma Sci.* **23**(6), 996 (1995)
16. A. Shyam, R.K. Rout, *IEEE Trans. Plasma Sci.* **25**(5), 1166–1168 (1997)
17. R. Niranjana, R.K. Rout, R. Srivastava, S.C. Gupta, *Indian J. Pure Appl. Phys.* **50**, 785–788 (2012)
18. H.R. Yousefi, G.R. Etaati, M. Ghorannevis, 31st EPS Conference on Plasma Phys. London, ECA vol 28G, P-5.006 (2004)
19. H. Yousefi, F.M. Aghamir, K. Masugata, *Phys. Lett. A* **361**, 360–363 (2007)
20. M. Milanese, R. Moroso, J. Pouzoa, *Eur. Phys. J. D* **27**, 77–81 (2003)
21. R. Shukla, S.K. Sharma, P. Banerjee, R. Das, P. Deb, T. Prabahar, B.K. Das, B. Adhikary, A. Shyam, *Rev. Sci. Instrum.* **81**, 083501 (2010)
22. S.M. Hassan, T. Zhang, A. Patran, R.S. Rawat, *Plasma Sour. Sci. Technol.* **15**(4), 614 (2006)
23. F.N. Beg, K. Krushelnick, C. Gower, S. Torn, A.E. Dangor, *Appl. Phys. Lett.* **80**(16), 3009 (2002)
24. H. Jafari, M. Habibi, *Eur. Phys. J. D* **68**, 234 (2014)
25. A. Serban, S. Lee, *J. Plasma Phys.* **60**(01), 021503 (1998)
26. R.K. Sharma, S.G. Chavan, R.K. Sadhu, S. Bhattacharya, G.P. Srivastava, *IEEE Trans. Plasma Sci.* **41**(10), 2666 (2013)
27. A.E. Abdou, M.I. Ismail, A.E. Mohamed, S. Lee, S.H. Saw, R. Verma, *IEEE Trans. Plasma Sci.* **40**(10), 2741 (2012)
28. J. Moreno, L. Birstein, R. Eayer, P.S.L. Soto, *Meas. Sci. Technol.* **19**, 087002 (2008)

Publisher's Note Springer Nature remains neutral with regard to jurisdictional claims in published maps and institutional affiliations.